

# MHD Convective Flow of Nano Fluids Over an Inclined Vertical Porous Surface

Dr. N.Srinivasa Rao

Associate Professor, Department of Mathematics, GFGC,kolar, Karnataka, India

Dr. Veeranna Y

Associate Professor, Department of Mathematics, government Science College ( Autonomous), Bangalore

**Abstract -** MHD boundary layer flow over a moving vertical porous surface with nanofluids under the influence of a uniform transverse magnetic field and heat radiation absorption effects has been brought out. Two different kinds of water-based nanofluids composed of  $Al_2O_3$  and  $TiO_2$  are adopted into deliberation. The governing equations for the flow are solved by making use of the Laplace transform method, and the solutions are displayed in closed form. The velocity, temperature, concentration, the shear stress, the rate of heat and mass transports near the surface has been described graphically for numerous values of the relevant parameters. The influence of important parameters such as Lewis number (Le), buoyancy ratio parameter (Nr), Brownian motion parameter (Nb), thermophoresis parameter (Nt), radiation(An), magneticfield(M) on velocity, temperature, concentration evaluation in the boundary layer region are examined in detailed. Furthermore the effects of these parameters on local Nusselt number (Nux), local Sherwood number (Shx) and local skin friction coefficient (Cf) are also investigated

**Keywords -** MHD flow, Inclined Plate; Magnetic field;FEM

## 1. INTRODUCTION

A nanofluid is a fluid containing small volumetric quantities of nanometer-sized particles, called nanoparticles. These fluids are envisioned to describe a fluid, in which nanometer-sized particles are suspended, in convectional heat transfer of basic fluids. The nanoparticles used in nanofluids are typically made of metals (Al, Cu), oxides ( $Al_2O_3$ ,  $CuO$ ,  $TiO_2$ ,  $SiO_2$ ), carbides ( $SiC$ ), nitrides ( $AlN$ ,  $SiN$ ), or nonmetals (graphite, carbon nanotubes). Nano particles are particles with a diameter of about 1-100 nm. Nano fluids commonly contain up to a 5% volume fraction of nanoparticles to see effective heat transfer enhancements of the base fluid. To improve the thermal conductivity of these fluids nano/micro-sized particle materials are suspended in liquids. Several theoretical and experimental researches have been made to enhance the thermal conductivity of these fluids; Choi [1] was the first among all who introduced a new type of fluid called nanofluid while doing research on new coolants and cooling technologies. Eastman et al. [2] have noticed in an experiment that the thermal conductivity of the base fluid (water) has increased up to 60% when  $CuO$  nano particles of volume fraction 5% are added to the base fluid. This is because of increasing surface area of the base fluid due to the suspension of nanoparticles. Heat transfer enhancement in electronic, aircraft, medical and experimental industries needs using efficient methods in equipment. In these industries, due to various dimensions of equipment, used systems do not have the capability of transferring critical heat flux caused by low effective methods. By using novel methods including mini channels and adding nanoparticles with higher thermal conductivity in cooling liquid, the advantages of utilizing novel heat transfer processes might be employed in an assortment of industries. Harmonized blends of nanoparticles composed of fundamental fluids are recognized as Nano fluids. The nano particles employed in nanofluids are utilized in inorganic-nano-tubes, diox-ides, materials and carbonisation. Base fluids consist of oil, ethy-lene glycol as well as water. These nano particles are also more significant in the specialties of aerospace and biomedical implications.

The MHD flows across the porous media and holds quite a lot of engineering and industrial challenges. Narayana [3], discussed to study the effects of radiation absorption and first-order chemical reaction on unsteady mixed convective flow of a viscous incompressible electrically conducting fluid through a porous medium of variable permeability between two long vertical non conducting wavy channels in the presence of heat generation. El bashbeshy et al. [4], addressed the results of heat radiation as well as magnetic field on unsteady combined convective flow along with heat transport through an exponentially stretching surface by suction in the existence of inside warmth production or else assimilation. Das et al. [5], discussed the transient natural convection in a vertical channel filled with nanofluids when thermal radiation is taken into consideration. Three dimensional natural convective MHD flow of nanofluid through porous linear stretching surface by the heat radiating phenomenon has been discussed by Nayak et al. [6]. Chamkha and Aly [7], investigated the numerical solution of steady natural convection boundary-layer flow of a nanofluid

consisting of a pure fluid with nanoparticles along a permeable vertical plate in the presence of magnetic field, heat generation or absorption, and suction or injection effects. Arifuzzaman et al. [8], investigated the modelling of an unsteady natural convective and higher order chemically reactive MHD fluid flow through a vertical oscillating porous plate with the effect of heat and radiation absorption. Combined effects of viscous dissipation and Joule heating on the combination of conduction and natural convection flow through a vertical flat surface have been explored by Alim et al. [9]., Ferdows et al. [10], addressed the consequences of Hall current as well as viscous dissipation on frontier stratum movement of temperature transport through a stretching surface. Over the past few days, Heat and mass transfer on unsteady MHD Oscillatory flow of blood through porous arteriole has been explained by Veera Krishna et al. [11]., Veera Krishna et al. [12], explored the heat and mass impacts on unsteady MHD fluctuated natural convection flow of second order fluid by porous medium during two perpendicular surfaces. Veera Krishna and Chamkha [13], addressed the Hall effects on unsteady MHD flow of second order fluid during porous medium through ramped wall temperature as well as ramped surface deliberation. Hakeem et al.[14], investigated second order MHD slip flow of nanofluid past a permeable surface. Baag et al. [15], examined entropy production investigation for MHD flow of visco-elastic fluid over an absorbent stretching sheet. Kalidas et al. [16], examined the flow of Jeffrey fluid through a stretching sheet with heat transfer and also surface slip. Veera Krishna and Chamkha [17], investigated the Hall and ion slip effects on the MHD convective flow of elastico-viscous fluid through porous medium between two rigidly rotating parallel plates with time fluctuating sinusoidal pressure gradient. The combined effects of Hall and ion slip on MHD rotating flow of ciliary propulsion of microscopic organism through porous medium have been studied by Veera Krishna et al. [18]., Seth et al. [19], discussed the numerical simulation of the New-tonian heating effect on unsteady MHD flow of Casson fluid past a flat vertical plate considering the impact of viscous dissipation, Joule heating, thermal diffusion, and nth order chemical reaction. Seth et al. [20], investigated unsteady MHD flow of a Casson fluid near a vertical oscillating plate through a non-Darcy porous medium and the impact of Joule heating, viscous dissipation, thermo-diffusion and Newtonian heating are taken into consideration. The investigation of simultaneous impact of Soret and Dufour effects on two-dimensional MHD free convective flow of an electrically conducting, viscous, and incompressible visco-elastic fluid over a non-linearly stretching surface with Navier's partial velocity slip boundary condition has been carried out by Seth et al. [21]., Seth et al. [22], explored the unsteady MHD natural convection flow of an optically thin, heat radiating, incompressible, viscous, chemically reactive, temperature dependent heat absorbing and electrically conducting fluid past an exponentially accelerated infinite vertical plate having ramped temperature, embedded in a porous medium considering the effects of Hall current and rotation. Bhattacharyya et al. [23], discussed the nature of two-dimensional MHD flow of an electro-conductive and thermally-radiating visco-elastic fluid past a non-linear stretching surface, considering viscous and Joule dissipation. The effects of Diffusion thermo, radiation absorption and chemical reaction on MHD free convective heat and mass transfer flow of a nanofluid bounded by a semi-infinite flat plate have been analyzed by Prasad et al. [24].,

Keeping on the top of the mentioned information, the investigation of the unsteady MHD boundary layer flow over a moving vertical porous surface with nanofluids in the presence of a uniform transverse magnetic field and heat radiation absorption effects has not been established yet.

## 2. MATHEMATICAL FORMULATION:

We consider a steady, laminar, two-dimensional, incompressible mixed convection boundary layer flow of a nanofluid along a semi-infinite inclined flat plate. The plate is embedded in a porous medium that is saturated with the same nanofluid, where the plate forms an acute angle, denoted as  $\alpha$ , with the vertical direction. In this study, we take into account the nanofluid model, which incorporates the influences of Brownian motion and thermophoresis. The nanofluid consists of a base fluid with nanoparticles suspended within it. The nanoparticles exhibit Brownian motion, which refers to their random movement due to collisions with fluid molecules. Additionally, the nanofluid experiences thermophoresis, which is the particle motion induced by temperature gradients. To establish a coordinate system for analysis, we define the x-direction as the distance measured along the surface of the plate, while the y-direction represents positions within the fluid. The surface of the plate is maintained at a uniform temperature,  $T_\infty$ , and concentration,  $C_\infty$ , both of which are higher than the ambient temperature and concentration.

The governing equations for this specific problem can be outlined as follows:

$$\frac{\partial u}{\partial x} + \frac{\partial v}{\partial y} = 0 \quad (1)$$

$$\frac{\partial p}{\partial y} = 0 \quad (2)$$

$$\mu_f \frac{1}{\kappa} u = -\frac{\partial p}{\partial x} + g [(1 - C_\infty) \rho_f \beta (T - T_\infty) - (\rho_p - \rho_f) (C - C_\infty)] \cos \cos \alpha - \frac{\sigma \beta_0^2}{\rho_f} u \quad (3)$$

$$\left( u \frac{\partial T}{\partial x} + v \frac{\partial T}{\partial y} \right) = \frac{k_m}{(\rho c)_f} \frac{\partial^2 T}{\partial y^2} + \frac{(\rho c)_p}{(\rho c)_f} \left[ D_B \frac{\partial C}{\partial y} \cdot \frac{\partial T}{\partial y} + \left( \frac{D_T}{T_\infty} \right) \left( \frac{\partial T}{\partial y} \right)^2 \right] - Q(T - T_\infty) - \frac{1}{(\rho c)_f} \cdot \frac{\partial}{\partial y} (q_r) \quad (4)$$

$$\frac{1}{\varepsilon} \left( u \frac{\partial C}{\partial x} + v \frac{\partial C}{\partial y} \right) = D_B \frac{\partial^2 C}{\partial y^2} + \left( \frac{D_T}{T_\infty} \right) \frac{\partial^2 T}{\partial y^2} \quad (5)$$

Depending upon the issue explanation, the boundary conditions are:

$$u = 0, \quad T = T_w, \quad C = C_w \text{ at } y = 0 \quad (6)$$

$$u = u_\infty, \quad T \rightarrow T_\infty, \quad C \rightarrow C_\infty \text{ at } y = \infty \quad (7)$$

Cross-differentiation can be employed to eliminate  $p$  from Eqs. (2) and (3), and the continuity Eq.(1) can be fulfilled by presenting a stream function  $\psi$ , which is defined as the Cauchy-Riemann equations:

$$u = \frac{\partial \psi}{\partial y}, \quad v = -\frac{\partial \psi}{\partial x} \quad (8)$$

By replacing Eq. (8) in Eqs. (3), (4), and (5), the three coupled similarity equations are:

$$\frac{\partial^2 \psi}{\partial y^2} = \left[ \frac{(1-C_\infty)\rho_{f\infty}\beta g k}{\mu} \frac{\partial T}{\partial y} - \frac{(\rho_p - \rho_{f\infty})g k}{\mu} \frac{\partial C}{\partial y} \right] \cos(\alpha) - \frac{\sigma \beta_o^2}{\rho} u \quad (9)$$

$$\frac{\partial \psi}{\partial y} \frac{\partial T}{\partial x} - \frac{\partial \psi}{\partial x} \frac{\partial T}{\partial y} = \frac{k_m}{(\rho c)_f} \frac{\partial^2 T}{\partial y^2} + \frac{\varepsilon(\rho c)_p}{(\rho c)_f} \left[ D_B \frac{\partial C}{\partial y} \frac{\partial T}{\partial y} + \left( \frac{D_T}{T_\infty} \right) \left( \frac{\partial T}{\partial y} \right)^2 \right] - Q(T - T_\infty) - \frac{1}{(\rho c)_m} \frac{\partial}{\partial y} (q_r) \quad (10)$$

$$\frac{1}{\varepsilon} \left( \frac{\partial \psi}{\partial y} \frac{\partial C}{\partial x} - \frac{\partial \psi}{\partial x} \frac{\partial C}{\partial y} \right) = D_B \frac{\partial^2 C}{\partial y^2} + \left( \frac{D_T}{T_\infty} \right) \frac{\partial^2 T}{\partial y^2} \quad (11)$$

The resulting similarity transformations are presented to simplify the mathematical analysis of the problem

$$\eta = \frac{y}{x} Pe_x^{\frac{1}{2}}, \quad f(\eta) = \frac{\psi}{\alpha_m Pe_x^{\frac{1}{2}}}, \quad \theta(n) = \frac{T - T_\infty}{T_w - T_\infty}, \quad \phi(n) = \frac{C - C_\infty}{C_w - C_\infty} \quad (12)$$

where,  $\alpha_m = \frac{k_m}{(\rho c)_f}$ . The radiation  $q_r$  through Rosseland approximation as

$$q_r = -\frac{4\sigma^*}{3K^*} \frac{\partial T^4}{\partial y} \quad (13)$$

where  $\sigma^*$  symbolizes the Stephan-Boltzmann constant and  $K^*$  symbolizes the mean absorption coefficient. We adopt that the temperature variations inside the circulation are with the value of  $T^4$  is a linear function of temperature. This is performed by extending  $T^4$  in a Taylor series around a free stream temperature  $T_\infty$  in the following manner:

$$T^4 = T_\infty^4 + 4T_\infty^3(T - T_\infty) + 6T_\infty^2(T - T_\infty)^2 + \dots \quad (14)$$

Ignoring higher-order terms in Eq. (19) past the first degree in  $(T - T_\infty)$ :

$$T^4 \cong 4T_\infty^3 T - 3T_\infty^4. \quad (15)$$

Thus, switching Eq. (20) to Eq. (18) will get

$$q_r = -\frac{16T_\infty^3 \sigma^*}{3K^*} \frac{\partial T}{\partial y}. \quad (16)$$

Using Eqs. (12) and (16), the governing non-linear partial differential equations i.e. Eqs. (9-11) together with boundary conditions i.e. Eqs. (6-7) reduced to momentum boundary layer equation as follows:

$$f'' = \frac{Ra_x}{Pe_x} (\theta' - Nr\varphi') \cos(\alpha) + Mf' \quad (17)$$

Thermal boundary layer equation:

$$\left(1 + \frac{4}{3}An\right)\theta'' + \frac{1}{2}f\theta' + Nb\theta'\phi' + Nt(\theta')^2 - Q\theta = 0 \quad (18)$$

Species diffusion boundary layer equations:

$$\phi'' + \frac{1}{2}Le\phi' + \frac{Nt}{Nb}\theta'' = 0 \quad (19)$$

The renovated boundary circumstances are

$$\eta = 0, \quad f = 0, \quad \theta = 1, \quad \phi = 1, \quad \eta \rightarrow \infty, \quad f' = 1, \quad \theta = 0, \quad \phi = 0. \quad (20)$$

Here prime implies  $\eta$  separation form, and the essential thermo physical factors influencing flow dynamics are described by

$$Nr = \frac{(\rho_p - \rho_{f\infty})(C_w - C_\infty)}{\rho_{f\infty}\beta(T_w - T_\infty)(1 - C_\infty)}, \quad Nb = \frac{\varepsilon\beta(\rho c)_p D_B(C_w - C_\infty)}{(\rho c)_f \alpha_m},$$

$$Nt = \frac{\varepsilon(\rho c)_p D_T(T_w - T_\infty)}{(\rho c)_f \alpha_m T_\infty}, \quad Le = \frac{\alpha_m}{\varepsilon D_B}, \quad Q = \frac{x^2}{Pe_x \alpha_m},$$

$$Ra_x = \frac{(1 - C_\infty)Kg\beta\rho_{f\infty}(T_w - T_\infty)x}{\mu\alpha_m},$$

$$Pe_x = \frac{U_\infty x}{\alpha_m}, \quad An = \frac{4T_\infty^3 \sigma^*}{K^* \alpha_m},$$

$$Ra = \frac{Ra_x}{Pe_x}, \quad M = \frac{\sigma\beta_o^2 x}{\rho Pe_x^{\frac{1}{2}}}$$

The problem at hand involves several important parameters that describe the characteristics of the nanofluid flow. These parameters include the Lewis number (Le), which represents the ratio of thermal diffusivity to mass diffusivity; the buoyancy ratio parameter (Nr), which accounts for the effect of buoyancy forces; the Brownian motion parameter (Nb), which captures the impact of nanoparticles' random motion; the thermophoresis parameter (Nt), which quantifies the particle motion induced by temperature gradients; the local Darcy-Rayleigh number (Ra\_x), which characterizes the combined effects of fluid flow and buoyancy forces; the local Peclet number (Pe\_x), which relates convective transport to molecular diffusion; the magnetic field parameter (M), which describes the influence of a magnetic field on the flow; the heat generation/absorption parameter (Q), which represents the amount of heat generated or absorbed in the system; and the thermal radiation parameter (An), which accounts for the radiative heat transfer. It's worth noting that porosity ( $\varepsilon$ ) is considered in the Nb, Nt, and Le parameters and is not directly modeled in this particular study. In this context, two important quantities of practical significance are the local Nusselt number ( $Nu_x$ ) and the local Sherwood number ( $Sh_x$ ). The local Nusselt number characterizes the convective heat transfer at a specific location, while the local Sherwood number quantifies the convective mass transfer. These numbers provide valuable insights into the heat and mass transfer phenomena occurring in the system under investigation.

$$Nu_x = \frac{xq_w}{k(T_w - T_\infty)}, \quad Sh_x = \frac{xq_m}{D_B(C_w - C_\infty)} \quad (21)$$

The heat flux and mass flux at the surface of the plate are represented by  $q_w$  and  $q_m$ , correspondingly. We get dimensionless representations of these essential design quantities using Eq. (17):

$$(Pe_x)^{\frac{-1}{2}}Nu_x = -\theta'(0), \quad (Pe_x)^{\frac{-1}{2}}Sh_x = -\phi'(0) \quad (22)$$

In the current context, the expressions  $(Pe_x)^{\frac{-1}{2}}Nu_x$  and  $(Pe_x)^{\frac{-1}{2}}Sh_x$  are denoted to as the compact Nusselt number and condensed Sherwood number, which are denoted by  $-\theta'(0)$  and  $-\phi'(0)$  respectively. Due to the highly nonlinear nature of the ordinary differential equations, i.e. Eqs.(17-19), analytical solutions are not feasible. Therefore, it is essential to choose an appropriate finite value for  $\eta_\infty$  in this numerical approach. The choice of an appropriate finite value for  $\eta_\infty$  is crucial in this numerical technique. To determine a suitable  $\eta_\infty$ , the solution process was initiated with  $\eta_\infty$ , and Eqs. (17-19) are resolved together with the boundary conditions (Eq. 20). The value of  $\eta_\infty$  was iteratively adjusted, continuing the solution process until further changes in  $\eta_\infty$  no longer affected the results. We confirmed that selecting  $\eta_{\max} = 8$  for temperature and  $\eta_{\max} = 5$  for concentration ensured that all numerical solutions converged to their asymptotic values under free stream conditions.

### 3.DISCSSION OF THE NUMERICAL RESULTS.

An exploration of the unsteady MHD boundary layer flow over an inspiring perpendicular surface by nanofluids in the presence of a uniform transverse magnetic field and heat radiation absorption phenomenon has been brought out. It discusses a clear insight on the physics of the problem, a parametric study is performed and the obtained computational results are elucidated through the help of graphical representations. Fig. 1 illustrates that the velocity of the fluid increases with an increase in Grashof number  $Gr$  for the cases of stationary plate as well as moving plate. This trend is due to the fact that the positive Grashof number  $Gr$  acts like a favourable pressure gradient which accelerates the fluid in the boundary layer. Consequently, the velocity increases with an increase in thermal Grashof number  $Gr$ . Grashof number ( $Gr$ ) that approximates the ratio of the buoyancy force to the viscous force acting. Therefore, the Grashof number represents the effect of free convection currents. Physically,  $Gr > 0$  means heating of the fluid or cooling of the boundary surface,  $Gr < 0$  means cooling of the fluid or heating of the boundary surface and  $Gr = 0$  corresponds to the absence of free convection. The contribution of absorption radiation parameters on the velocity profiles is noticed in Fig.2.

The Fig. 3 (a-d) revealed that the fluid temperature profiles for the two types of water-based nanofluids  $Al_2O_3$ -water and  $TiO_2$  - water. However, due to higher thermal conductivity of  $Al_2O_3$ -water nanofluids, the temperature of  $Al_2O_3$ -water nanofluid is found to be higher than  $TiO_2$ -water nanofluids. It is also seen that the thermal boundary layer thickness is more for  $Al_2O_3$ -water than  $TiO_2$ -water nanofluids. The Fig. 9 (a) displayed the effect of volume fraction  $\phi$  of nanoparticles on the temperature distribution. The fluid temperature increases as volume fraction parameter  $\phi$  enlarges. Also, the thermal boundary layer for  $Al_2O_3$ -water is greater than for pure water ( $\phi=0$ ). This is because  $Al_2O_3$  has high thermal conductivity and its addition to the water based fluid increases the thermal conductivity for the fluid, so the thickness of the thermal boundary layer increases. It is also observed that with increasing the volume fraction  $\phi$  of the nanoparticles the thermal boundary layer is increased. This agrees with the physical behavior of nanoparticles. This observation shows that the use of nanofluids will be significance in the cooling and heating processes. Fig.3(b) also represents the variation of nanofluid temperature for Prandtl number  $Pr$ . The temperature profiles exhibit that the fluid temperature decreases as  $Pr$  increases. This is due to the fact that a higher Prandtl number fluid has relatively low thermal conductivity, which reduces conduction and thereby the thermal boundary layer thickness; and as a result, temperature decreases. The fluid temperature is high near the plate and decreases asymptotically to the free stream with zero-value far away from the plate. From Fig. 3(c) displayed the effect of radiation parameter  $Nr$  on the temperature delivery. The increase in radiation parameter means the release of heat energy from the flow region and so the fluid temperature decreases. A decrease in the values of  $Nr$  for given  $k\eta$  and  $T_1$  means a decrease in the Rosseland radiation absorption. Since divergence of the radiative heat flux increases, radiation absorption decreases which in turn causes an increase in the rate of radiative heat transfer to the fluid and hence the fluid temperature increases. This represents that, the thermal boundary layer decreases and more uniform temperature distribution across the boundary layer. The temperature increases with increasing radiation absorption parameters (Fig. 3(d)). This is due to the fact that when heat is absorbed, the buoyancy forces accelerate the flow and temperature of the fluid. The consequence of radiation parameter  $Nr$  on the velocity profiles is presented in Fig. 4. The fluid velocity enhances as the value of  $Nr$  increases for both cases of stationary plate as well as moving plate. The velocity profiles increase sharply near the surface of the plate and after attaining respective utmost, the curves settle down to the corresponding asymptotic value. Therefore,  $Nr$  behaves like a supporting force which accelerates the fluid particles near the vicinity of the plate. Also, it is noted that momentum boundary layer thickness increases when  $Nr$  tends to increase inside a boundary layer region.

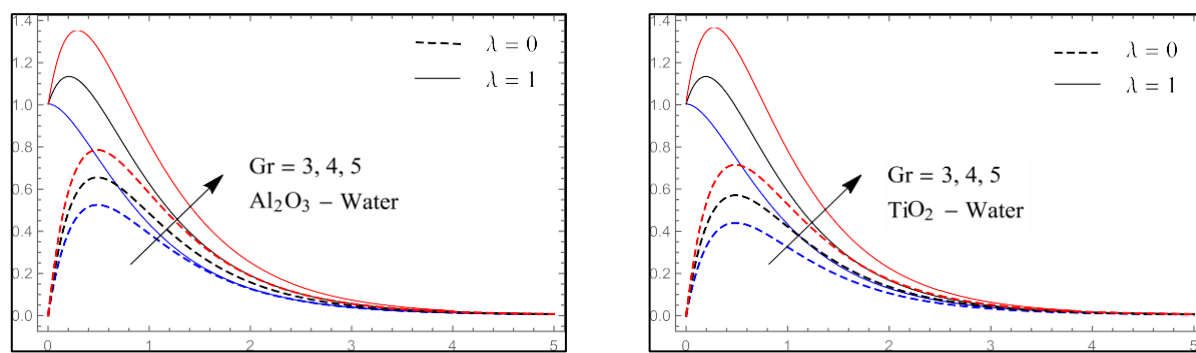
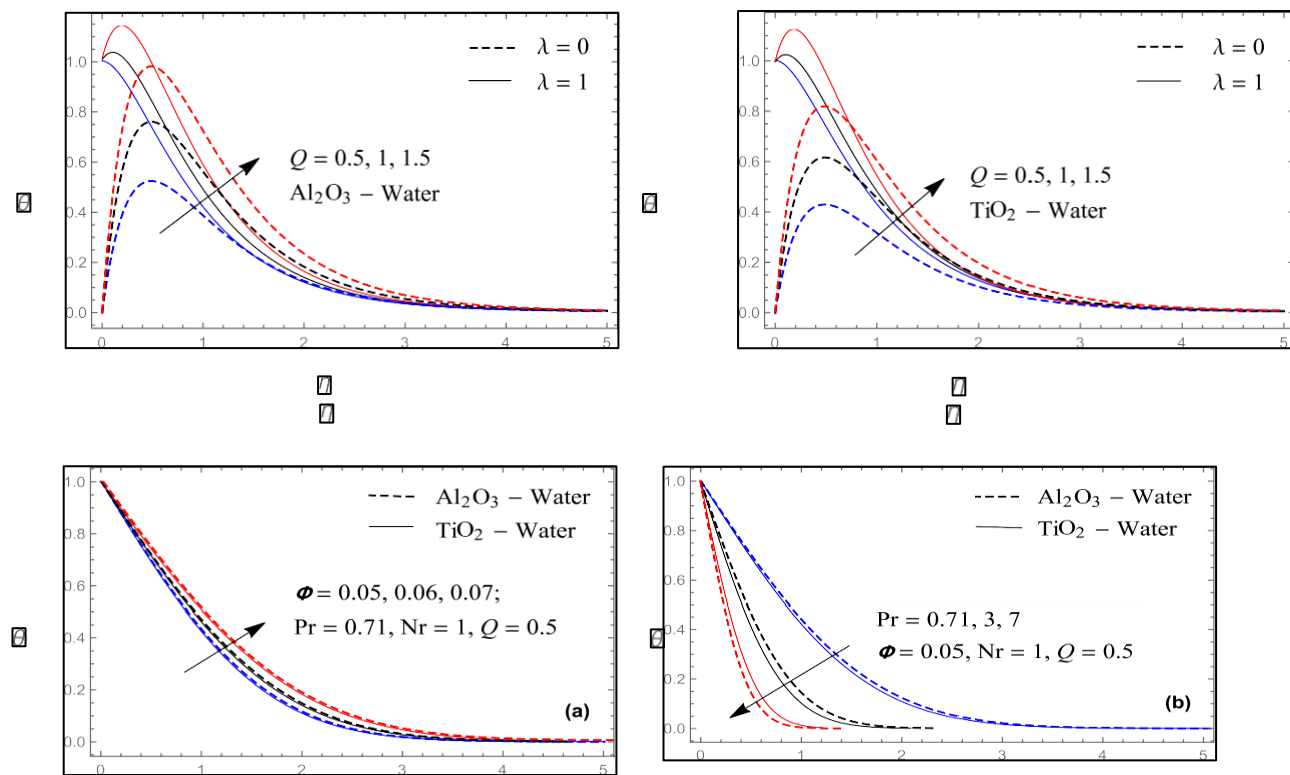
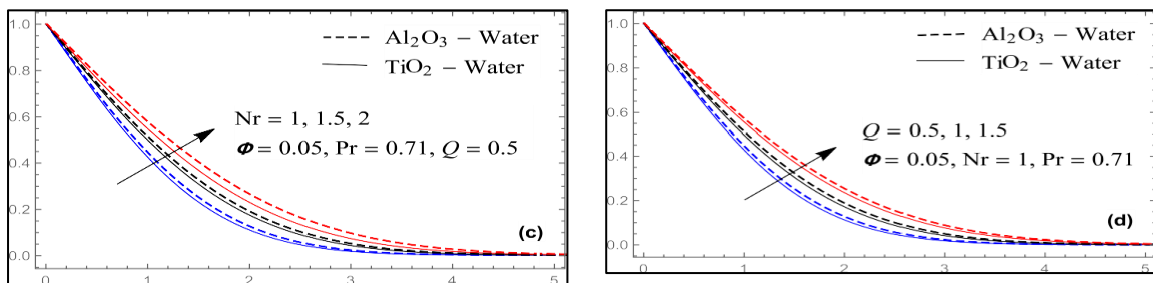


Fig.1 velocity profiles for  $u$  against  $Gr$  with  $M=2, K=0.5, Nr=0.5, u=0.05, Q=0.5, t=0.1$ .



Fig.2 velocity profiles for  $u$  against  $Q$  with  $M=2, K=0.5, Nr=0.5, u=0.05, Gr=3, t=0.1$ .Fig.3. Temperature profiles for  $h$  against  $u, Pr, Nr$  and  $Q$ .Fig.4 velocity profiles for  $u$  against  $Nr$  with  $M=2, K=0.5, u=0.05, Gr=3, Q=0.5, t=0.1$ .Table.1. Variation of  $Nur$  and  $Shr$  with  $Pr$ ,  $Nb$  and  $Nr$  for  $Nt= 0.1$ ,  $Nc = 10$  and  $Le = 10$ .

$N_b$	$N_r$	$P_r=1$		$P_r=5$		$P_r=10$	
		$Nu$	$Sh$	$Nu$	$Sh$	$Nu$	$Sh$
0.1	0.1	0.6916	0.8338	0.5223	1.5182	0.3586	1.5522
	0.2	0.6884	0.8207	0.5189	1.5051	0.355	1.5392
	0.3	0.6851	0.8069	0.5152	1.4914	0.3513	1.5256
	0.4	0.6817	0.7924	0.5115	1.4771	0.3475	1.5113
	0.5	0.6781	0.7772	0.5075	1.4621	0.3435	1.4964
	0.6	0.6742	0.761	0.5034	1.4462	0.3393	1.4807
	0.7	0.6702	0.7437	0.499	1.4294	0.3349	1.4641
	0.8	0.6489	0.8945	0.4756	1.5801	0.3107	1.6145
0.3	0.1	0.6468	0.8827	0.4732	1.5685	0.3083	1.6031
	0.2	0.6446	0.8705	0.4708	1.5566	0.3058	1.5912
	0.3	0.6422	0.8577	0.4682	1.5441	0.3032	1.5789
	0.4	0.6398	0.8444	0.4656	1.5311	0.3005	1.5661
	0.5	0.6373	0.8304	0.4629	1.5176	0.2978	1.5527
	0.6	0.6347	0.8157	0.46	1.5034	0.2949	1.5387
	0.7	0.6319	0.8001	0.457	1.4885	0.2919	1.524

	0.8	0.608	0.9094	0.4305	1.5963	0.2644	1.6312
0.5	0.1	0.6063	0.8981	0.4286	1.5852	0.2625	1.6202
	0.2	0.6045	0.8863	0.4266	1.5737	0.2605	1.6088
	0.3	0.6027	0.874	0.4246	1.5618	0.2585	1.597
	0.4	0.6008	0.8612	0.4225	1.5494	0.2564	1.5848
	0.5	0.5988	0.8477	0.4204	1.5364	0.2542	1.572
	0.6	0.5968	0.8337	0.4181	1.5229	0.2519	1.5587
	0.7	0.5946	0.8188	0.4158	1.5088	0.2496	1.5448
	0.8	0.355	-0.149	0.145	0.47	-0.03	0.485

Table.2. Variation of Nu and Sh with Le, Nb and Nr for Nt =0.1, Nc =10 and Pr=10.

Nb	Nr	Le = 1		Le = 5		Le = 10	
		Nu	Sh	Nu	Sh	Nu	Sh
0.1	0.1	0.7196	1.3504	0.5382	1.5288	0.6488	1.54518
	0.2	0.7166	1.3378	0.5348	1.5162	0.6454	1.53268
	0.3	0.7134	1.3247	0.5314	1.5031	0.6418	1.51968
	0.4	0.7101	1.3109	0.5277	1.4894	0.6381	1.50608
	0.5	0.7067	1.2964	0.524	1.4751	0.6343	1.49178
	0.6	0.7031	1.2812	0.52	1.4601	0.6303	1.47688
	0.7	0.6992	1.265	0.5159	1.4442	0.6261	1.46118
	0.8	0.6952	1.2477	0.5115	1.4274	0.6217	1.44458
0.3	0.1	0.6739	1.3985	0.4881	1.5781	0.5975	1.59498
	0.2	0.6718	1.3867	0.4857	1.5665	0.5951	1.58358
	0.3	0.6696	1.3745	0.4833	1.5546	0.5926	1.57168
	0.4	0.6672	1.3617	0.4807	1.5421	0.59	1.55938
	0.5	0.6648	1.3484	0.4781	1.5291	0.5873	1.54658
	0.6	0.6623	1.3344	0.4754	1.5156	0.5846	1.53318
	0.7	0.6597	1.3197	0.4725	1.5014	0.5817	1.51918
	0.8	0.6569	1.3041	0.4695	1.4865	0.5787	1.50448
0.5	0.1	0.633	1.4134	0.443	1.5943	0.5512	1.61168
	0.2	0.6313	1.4021	0.4411	1.5832	0.5493	1.60068
	0.3	0.6295	1.3903	0.4391	1.5717	0.5473	1.58928
	0.4	0.6277	1.378	0.4371	1.5598	0.5453	1.57748
	0.5	0.6258	1.3652	0.435	1.5474	0.5432	1.56528
	0.6	0.6238	1.3517	0.4329	1.5344	0.541	1.55248
	0.7	0.6218	1.3377	0.4306	1.5209	0.5387	1.53918

	0.8	0.6196	1.3228	0.4283	1.5068	0.5364	1.52528
--	-----	--------	--------	--------	--------	--------	---------

The data in Table .1 indicate how the reduced Nusselt and Sherwood numbers are affected by the changes in the Prandtl number Pr, the Brownian motion parameter Nb and the buoyancy parameter Nb when the rest of the parameters are fixed at the values indicated in the table heading. For every combination of Nb and Nr, both the reduced Nusselt and reduced Sherwood numbers increase with the increase in Pr. For a fixed Pr, both the reduced Nusselt number and the reduced Sherwood number decrease as Nb and Nr each increase. Table .2 allows the reader to see how the changes in the Lewis affect the reduced Nusselt number and the reduced Sherwood number. As the Lewis number increases the reduced Nusselt number increases slightly but there is a substantial increase in the reduced Sherwood number. Tables.1 and 2 provide information about the heat and mass transfer characteristics of the flow in a form convenient for research and engineering calculations.

#### 4. REFERENCES.

- [1] Choi S.U.S,Enhancing thermal conductivity of fluids with nanoparticles, developments and applications of non-Newtonian flows, in: D.A. Siginer, H.P. Wang (Eds.), FED—Vol. 231/MD, Vol. 66, The American Society of Mechanical Engineers, New York, (1995).99-105
- [2] Eastman. J.A, Choi. S.U.S, Li.S, Thompson.L.J.andLee.S, Enhanced thermal conductivity through the development of nanofluids, in: S. Komarneni, J.C. Parker, H.J. Wollenberger (Eds.), Nanophase and Nanocomposite Materials II, MRS, Pittsburg, PA, 1997.3-11
- [3] Narayana PVS. Effects of variable permeability and radiation absorption on MHD mixed convective flow in a vertical wavy channel with travelling thermal waves. *Propul Power Res* 2015;4(3):150–60. doi: <https://doi.org/10.1016/j.jppr.2015.07.002>.
- [4] Elbashbeshy EMA, Eram TG, Abdelgaber KM. Effects of thermal radiation and magnetic field on unsteady mixed convection flow and heat transfer over an exponentially stretching surface with suction in the presence of internal heat generation/absorption. *J Egyptian Math Soc* 2012;20:215–22.
- [5] Das S, Jana RN, Makinde OD. Transient natural convection in a vertical channel filled with nanofluids in the presence of thermal radiation. *Alex Eng J* 2016;55:253–62. doi: <https://doi.org/10.1016/j.aej.2015.10.013> 1110-0168.
- [6] Nayak MK, Akbar NS, Pandey VS, Khan ZH, Tripathi D. 3D free convective MHD flow of nanofluid over permeable linear stretching sheet with thermal radiation. *Powder Tech* 2017;315:205–15.
- [7] Chamkha AJ, Aly AM. MHD free convection flow of a nanofluid past a vertical plate in the presence of heat generation or absorption effects. *Chem Eng Commun* 2011;198(3):425–41. doi: <https://doi.org/10.1080/00986445.2010.520232>.
- [8] Arifuzzaman SM, Khan MS, Mehedi MFU, Rana BMJ, Ahmed SF. Chemically reactive and naturally convective high speed MHD fluid flow through an oscillatory vertical porous plate with heat and radiation absorption effect. *Eng Sci Tech An Int J* 2018;21:215–28. doi: <https://doi.org/10.1016/j.jestch.2018.03.004>.
- [9] Alim MA, Alam MM, Mamun AA, Hossain B. Combined effect of viscous dissipation and Joule heating on the coupling of conduction and free convection along a vertical flat plate. *Int Commun Heat Mass Transf* 2008;2008(35):338–46.
- [10] Ferdows M, Afify AA, Tzirtzilakis EE. Hall current and viscous dissipation effects on boundary layer flow of heat transfer past a stretching sheet. *Int J Appl Compu Math* 2017;3(4):3471–87.
- [11] Veera Krishna M, Swarnalathamma BV, Prakash J. Heat and mass transfer on unsteady MHD Oscillatory flow of blood through porous arteriole. *Appl Fluid Dynam, Lect Notes Mech Eng* 2018;22:207–24. doi: [https://doi.org/10.1007/978-981-10-5329-0\\_14](https://doi.org/10.1007/978-981-10-5329-0_14).
- [12] Veera Krishna M, Subba Reddy G, Chamkha AJ. Hall effects on unsteady MHD oscillatory free convective flow of second grade fluid through porous medium between two vertical plates. *Phys Flu* 2018;30:. doi: <https://doi.org/10.1063/1.5010863023106>.
- [13] Veera Krishna M, Chamkha AJ. Hall effects on unsteady MHD flow of second grade fluid through porous medium with ramped wall temperature and ramped surface concentration. *Phys Flu* 2018;30:. doi: <https://doi.org/10.1063/1.5025542053101>.
- [14] Hakeem AK, Vishnu Ganesh N, Ganga B. Magnetic field effect on second order slip flow of Nano fluid over a stretching/shrinking sheet with thermal radiation effect. *J Magn Magn Mat* 2015;381:243–57. doi: <https://doi.org/10.1016/j.jmmm.2014.12.010>.
- [15] Baag S, Mishra SR, Dash GC, Acharya MR. Entropy generation analysis for viscoelastic MHD flow over a stretching sheet embedded in a porous medium. *Ain Shams Eng J* 2016;8(4):623–32. doi: <https://doi.org/10.1016/j.asej.2015.10.017>.
- [16] Kalidas D, Nilangshu Acharya, Prabir Kumar Kundu, Radiative flow of MHD Jeffrey fluid past a stretching sheet with surface slip and melting heat transfer. *Alex Eng J* 2015;54(4):815–21. doi: <https://doi.org/10.1016/j.aej.2015.06.008>.
- [17] Veera Krishna M, Chamkha AJ. Hall and ion slip effects on MHD rotating flow of elastico-viscous fluid through porous medium. *Int Commun Heat Mass Transf* 2020;113:. doi: <https://doi.org/10.1016/j.icheatmasstransfer.2020.10.4494104494>.
- [18] Veera Krishna M, Sravanthi CS, Gorla RSR. Hall and ion slip effects on MHD rotating flow of ciliary propulsion of microscopic organisms through porous media. *Int Commun Heat Mass Transf* 2020;112:. doi: <https://doi.org/10.1016/j.icheatmasstransfer.2020.104500104500>.
- [19] Seth GS, Bhattacharyya A, Kumar R, Mishra MK. Modelling and numerical simulation of hydromagnetic natural convection Casson fluid flow with n-thorder chemical reaction and Newtonian heating in porous medium. *J Porous Media* 2019;22(9):1141–57. doi: <https://doi.org/10.1615/JPorMedia.2019.025699>.
- [20] Seth GS, Kumar R, Tripathi R, Bhattacharyya A. Double diffusive MHD Casson fluid flow in a non-Darcy porous medium with Newtonian heating and thermo-diffusion effects. *Int J Heat Tech* 2018;36(4):1517–27. doi: <https://doi.org/10.18280/ijht.360446>.
- [21] Seth GS, Bhattacharyya A, Mishra MK. Study of partial slip mechanism on free convection flow of viscoelastic fluid past a non-linearly stretching surface. *Comput Thermal Sci: An Int J* 2019;11(1–2):105–17. doi: <https://doi.org/10.1615/ComputThermalSci.2018024728>.
- [22] Seth GS, Bhattacharyya A, Tripathi R. Effect of Hall current on MHD natural convection heat and mass transfer flow of rotating fluid past a vertical plate with ramped wall temperature. *Front Heat Mass Transf* 2017;21:1–12. doi: <https://doi.org/10.5098/hmt.9.21>.
- [23] Bhattacharyya A, Seth GS, Kumar R. Modeling of visco-elastic fluid flow past a non-linearly stretching surface with convective heat transfer: OHAM Analysis. *Math Model Sci Compu Appl* 2020;308:297–312. doi: [https://doi.org/10.1007/978-981-15-1338-1\\_22](https://doi.org/10.1007/978-981-15-1338-1_22).
- [24] M. Veera Krishna, N. Ameer Ahamad and A.J. Chamkha *Ain Shams Engineering Journal* 12 (2021). 3043–3056